Available online at www.sciencedirect.com

Journal of Applied Research and Technology

Journal of Applied Research and Technology 15 (2017) 102–109

www.jart.ccadet.unam.mx

Original

Enhancement of $GdVO_4$:Eu3+ red fluorescence through plasmonic effect of silver nanoprisms on Si solar cell surface

Swati Bishnoi, Santa Chawla *

Luminescent Materials Group, CSIR-National Physical Laboratory, Dr. K.S. Krishnan Road, New Delhi 110012, India

Received 30 August 2016; accepted 10 January 2017
Available online 27 March 2017

Abstract

A comprehensive study on deposition and conjugation of red emitting phosphor ($GdVO_4$:Eu^{3+}) and silver nanoprisms (Ag NP) on commercial single crystal silicon solar cell surface has been done to establish the optimum dielectric separating layer (PVA) sequence between consecutive species through confocal fluorescence mapping and spectroscopy. Results show that up to 310% fluorescence enhancement could be achieved in optimal arrangement of emitter, PVA and Ag NP layers on Si cell surface. The current work shows the potential of plasmon enhanced down shifting fluorescence of rare-earth doped vanadate in enhancing performance of SiPV devices.

Keywords: Plasmon enhanced fluorescence; Rare earth doped phosphor; Metal nanoparticles

1. Introduction

Solar spectrum conversion through phosphors is a potential option for utilizing the ultraviolet (UV) and infrared (IR) part of the solar spectrum that otherwise remains unutilized by existing silicon solar cells. Silicon solar cells have inherent lower spectral response in the ultraviolet-blue (300–450 nm) region because of its band gap (1.1 eV) and fast surface recombination, high reflectance and thermalization losses of high energy photons (Shalav, Richards, Trupke, Krämer, & Güdel, 2005). Such losses may be minimized by using a down shifting (DS) phosphor layer which can convert a portion of the incident high energy UV photons to the visible region, where the Si solar cell has optimum spectral response (Chawla, Parvaz, Kumar, & Buch, 2013; Richards, 2006). Solar UV photons are absorbed near the Si cell surface which leads to the recombination of photo-generated electrons with surface defects, lowering the short wavelength spectral response. A DS phosphor layer on the Si surface can readily absorb UV photons and give fluorescence of lower energy photons that can be absorbed deep within the solar cell, close to the depletion region thus enhancing the collection efficiency. The red spectral region offers an optimum balance in the penetration depth and spectral response of Si cell. The development of suitable phosphors with high luminescence efficiency and integration of phosphor layer with Si solar cell is a daunting task. Rare earth-doped red-emitting phosphors, particularly Eu^{3+} doped vanadates (Gavrilović, Jovanović, Lojpur, & Dramićanin, 2014; Khan et al., 2008) and oxides (Dai, Foley, Breshike, Lita, & Strouse, 2011; Jayaramaiah, Lakshminarasappa, & Nagabhushana, 2012; Yadav et al., 2009) have shown very high luminescence efficiency. There are few reports on the direct deposition of phosphor layer on Si cell surface with dye (Klampaftis, Congiu, Robertson, & Richards, 2011), inorganic rare earth-doped phosphors (Yen-Chi, Woan-Yu, & Teng-Ming, 2011; Chen & Chen, 2011). Enhancement in Si cell efficiency by using Eu^{3+} complexes doped polyvinyl acetate (PVA) film (Liu et al., 2013; Le Donne, Acciarri, Narducci, Marchionna, & Binetti, 2009) and a layer of YVO_4:Bi^{3+}, Eu^{3+} nanophosphors (Huang et al., 2013) are reported. Recently there have been reports on the improvement in the performance of Si solar cells using nanostructured YVO_4:Eu^{3+} downshifting phosphor layer (Chander et al., 2015; Kumar, Khan, & Chawla, 2013).

Gadolinium orthovanadate ($GdVO_4$)-based materials have gained attention because of their interesting luminescent and

* Corresponding author.
E-mail address: sntchawla@yahoo.com (S. Chawla).

Peer Review under the responsibility of Universidad Nacional Autónoma de México.

http://dx.doi.org/10.1016/j.jart.2017.01.007

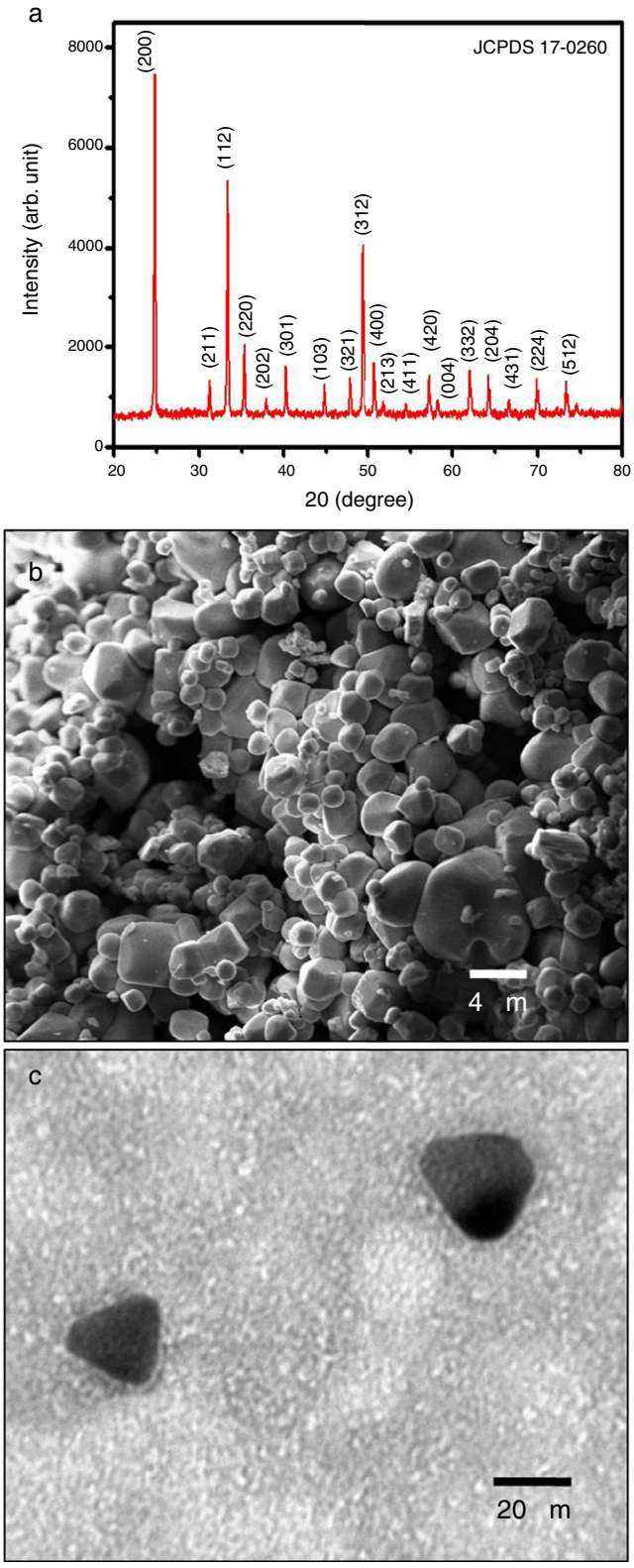

Fig. 1. (a) X-ray powder diffraction spectrum of $GdVO_4:Eu^{3+}$; (b) SEM image of $GdVO_4:Eu^{3+}$; (c) TEM image of Ag nanoprisms.

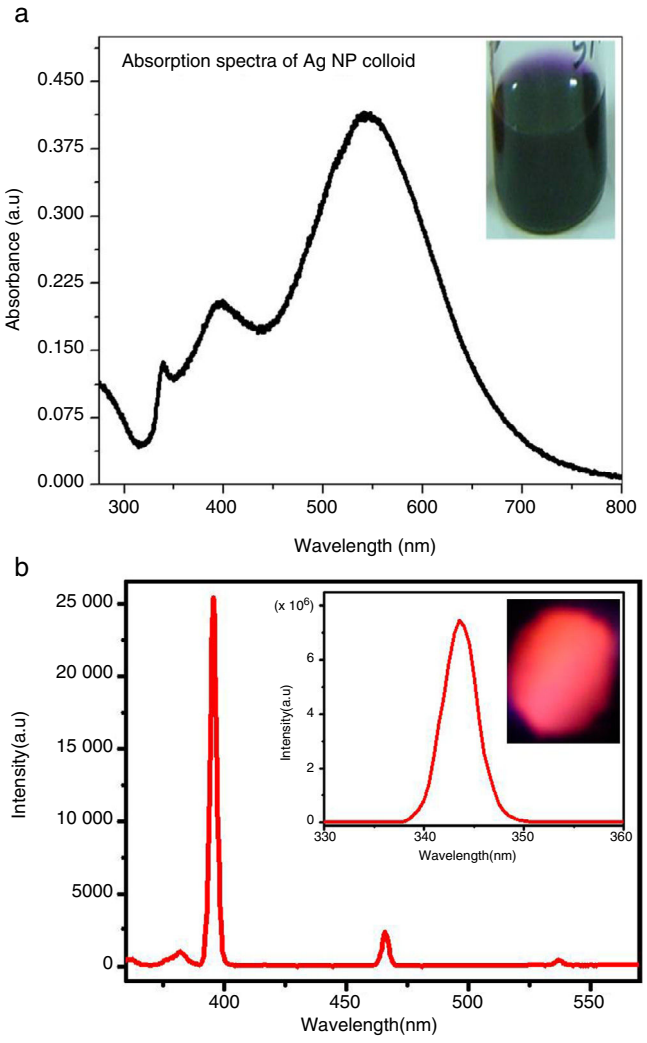

Fig. 2. (a) UV-visible absorption spectrum of Ag NP colloid, the inset shows the violet colloid of Ag nanoprisms; (b) PL excitation spectra at red emission, the inset shows the charge transfer excitation band at 343 nm and the digital photograph of the $GdVO_4:Eu^{3+}$ powder sample under UV excitation.

magnetic properties. Gd compounds doped with luminescent lanthanide ions can be efficiently excited with UV radiation because of the strong absorption of the VO_4^{3-} groups and efficient energy transfer from $GdVO_4$ to lanthanide ions. Therefore, Eu^{3+}, Dy^{3+}, Sm^{3+} doped $GdVO_4$ are widely used as phosphor (Singh et al., 2012).

Recent reports suggest that metal enhanced fluorescence is a viable option for further enhancement of rare earth (RE) emissions (Bishnoi, Das, & Chawla, 2014; Feng, Sun, & Yan, 2009) but optimal conjugation of phosphor and metal nanoparticles (MNP) is a challenge since surface plasmon resonance (SPR) of MNPs depend upon their shape, size and surrounding dielectric environment. However, contradictory reports exist in literature regarding efficiency enhancement of silicon solar cells by plasmonic effects including metal nanostructures (El Daif et al., 2012; Thouti, Sharma, Sardana, & Komarala, 2014; Wan et al., 2010) degrading the device's performance. Most reports on plasmon-enhanced fluorescence are on glass/quartz substrate (Buch, Kumar, Mamgain, & Chawla, 2013). A

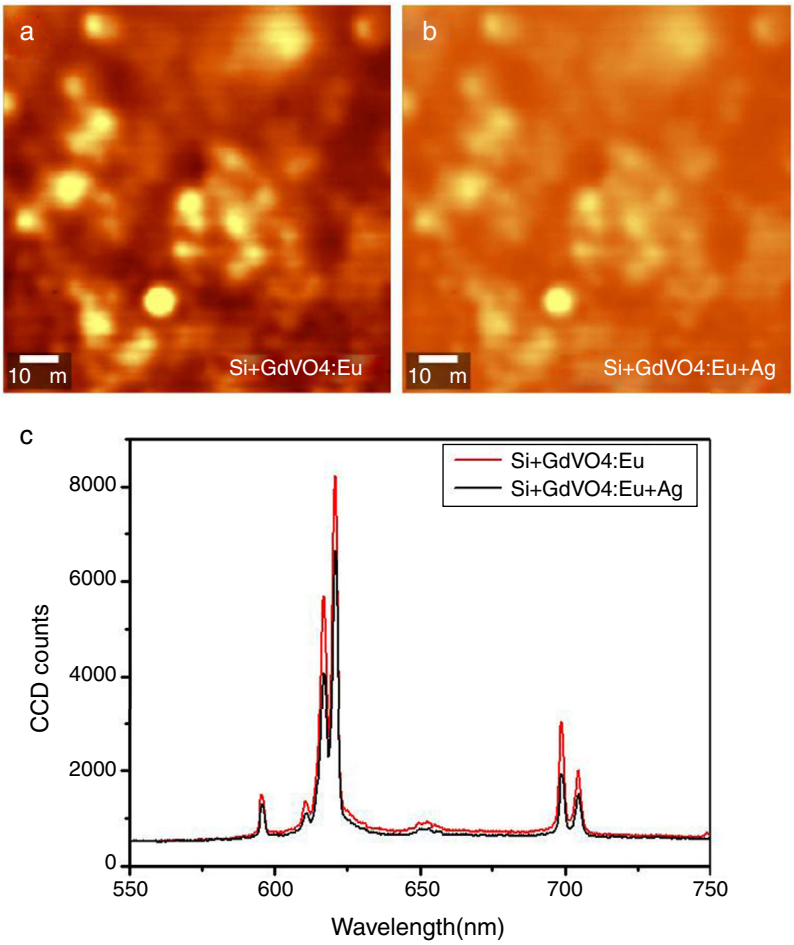

Fig. 3. Confocal fluorescence map of (a) $GdVO_4$:Eu; (b) $GdVO_4$:Eu + Ag NP deposited on the Si cell; (c) corresponding spectra comparing the Eu^{3+} emission intensity with and without Ag NPs suggesting quenching of fluorescence.

dielectric intervening layer between phosphor and MNPs play a crucial role in enhancing or quenching (Anger, Bharadwaj, & Novotny, 2006; Wang et al., 2011a; Wang et al., 2011b) fluorescence from phosphor material. Since optimum conjugation of substrate, phosphor and MNPs are crucial to perform plasmon enhanced fluorescence, it is extremely important to evolve the conjugation sequence on the Si solar cell surface. We have chosen an intense red-emitting phosphor $GdVO_4:Eu^{3+}$ with excitation range in the UV-blue region. Ag nanoprisms are chosen since they can strongly confine and enhance the EM field in the visible region because of their ability to exhibit distinct dipolar and quadrupolar resonances (Hao & Schatz, 2004) which can be tuned in the UV-visible region that can play an important role in fluorescence enhancement of RE ions (Wang et al., 2011a; Wang et al., 2011b). Polyvinyl alcohol (PVA) has been chosen as the spacer layer as it has been reported that a PVA layer on the Si cell surface does not change the cell's performance (Liu et al., 2013) and Eu^{3+}-doped PVA layer on the Si cell has been shown to improve external quantum efficiency in the UV spectral region (Guedje, Giloan, Potara, Hounkonnou, & Astilean, 2012). We have done a systematic study of conjugating $GdVO_4:Eu^{3+}$ phosphor and silver nanoprisms so that maximum fluorescence enhancement could be realized on commercial Si solar cell surface.

2. Experimental methods

$GdVO_4:Eu^{3+}$ was synthesized using a controlled solid state reaction method. For the synthesis of Eu (5%)-doped $GdVO_4$ particles, analytical grade commercial Gd_2O_3 (99.99% pure), V_2O_5 and Eu_2O_3 (99.99% pure) have been used. The precursor materials were taken in their stoichiometric ratios, mixed thoroughly, packed in recrystallized alumina boat and fired at 1000 °C for 2 h in air atmosphere. The resulting product was allowed to cool slowly at room temperature and was crushed to a fine powder using mortar and pestle.

A silver nanoparticle solution was prepared by following the method by Heredia (2011). The silver precursor used was $AgNO_3$ in which poly vinyl pyrrolidone was added followed by trisodium citrate ($Na_3C_6H_5O_7$) with continuous stirring. A solution of $NaBH_4$ was added for reduction of silver salt to Ag^+ followed by the formation of spherical Ag nanoparticles which were etched with H_2O_2 solution (30% w/v) to form silver nanoprisms.

A paste of phosphor $GdVO_4:Eu^{3+}$ with the consistency of paint was prepared in an appropriate amount (1 g) of polymethyl methacrylate (PMMA) dissolved in 5 ml dichloro methane. A dilute solution (3%) of polyvinyl alcohol (PVA) was prepared in DI water to be used as an intervening

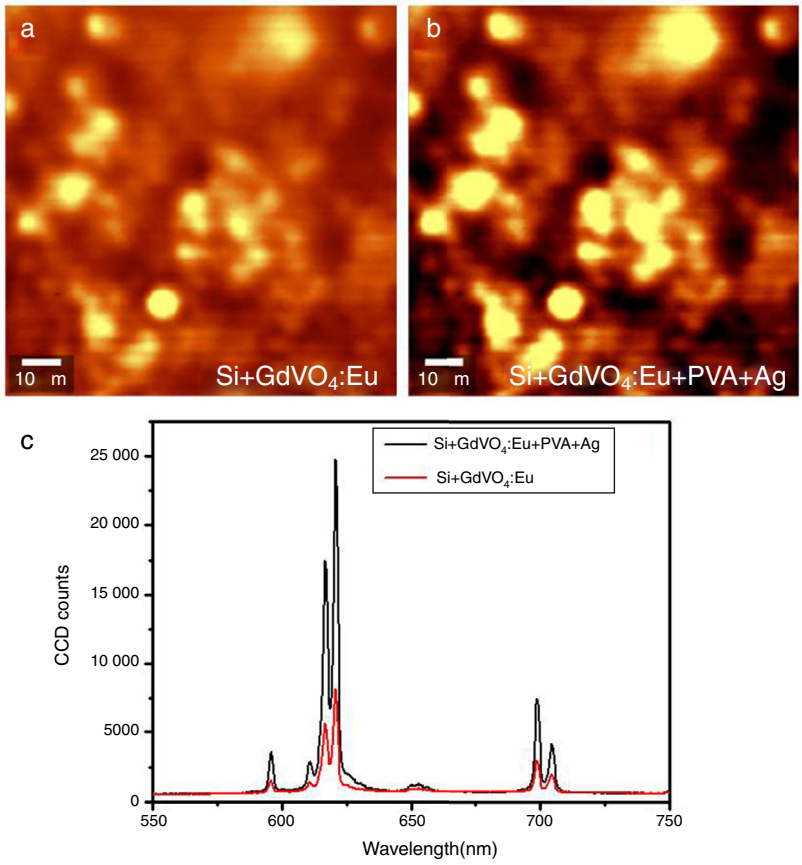

Fig. 4. Confocal fluorescence map of (a) $GdVO_4$:Eu; (b) $GdVO_4$:Eu + PVA + Ag NP deposited on the Si cell; (c) corresponding spectra comparing the Eu^{3+} emission intensity with and without Ag NPs suggesting enhancement of fluorescence.

dielectric layer. The sequence of deposition of phosphor paint on single crystal Si solar cell (with lab tested efficiency of 13.6%), Ag NP colloidal solution and PVA solution on Si solar cell surface were varied in four different ways to optimize maximum fluorescence enhancement. The sequences adopted were (1) Si cell + $GdVO_4$:Eu^{3+} + AgNP; (2) Si cell + $GdVO_4$:Eu^{3+} + PVA + Ag NP; (3) Si Cell + PVA + $GdVO_4$:Eu^{3+} + Ag NP; (4) Si cell + PVA + $GdVO_4$:Eu^{3+} + PVA + Ag NP. Controlled drop casting of individual species followed by drying was harnessed for sequential deposition. The dielectric PVA layer was used to separate different species and to investigate the effect of an intervening dielectric layer on the fluorescence output from $GdVO_4$:Eu^{3+}.

2.1. Characterization

The X-ray powder diffraction (XRD) of the Eu doped $GdVO_4$ powdered sample was carried out on a Rigaku miniflex X-ray diffractometer with Cu-Kα radiation (1.54 Å). The morphology of the powdered sample was inspected using a LEO 440 PC digital scanning electron microscope (SEM). The absorption spectra of the Ag NP solution was measured using Avantes UV-visible spectrometer. The photoluminescence (PL) characteristics were studied under a WITec Confocal fluorescence microscope (WITec 300 M^+) with PL mapping facility. Confocal fluorescence mapping and spectroscopy of the identical area was done of the bare Si cell and after each stage of deposition of $GdVO_4$:Eu^{3+} and Ag NP solution and also PVA in samples (2–4) as mentioned above. A specific area of the cell was chosen under a 20× objective in the confocal microscope. Starting from the bare Si cell, confocal measurements were done for all 4 sets of layered structures and fluorescence distribution was recorded under excitation of a UV diode laser (λ ∼ 375 nm, output power 10 mW, Toptica). Confocal fluorescence mapping and spectroscopy was done on the Si cell with sequence of layers deposited on it. In order to investigate the plasmonic effect on the red emission from Eu^{3+} doped in $GdVO_4$ particles with various layer sequence of intervening PVA layer, the same area of the Si cell was used in each set, without disturbing the Si cell position on the confocal microscope sample plate. Spacer layer of PVA, phosphor layer and Ag NP layer was deposited on the Si cell surface by drop casting keeping the Si cell position fixed.

3. Results and discussion

3.1. XRD, SEM AND TEM

The synthesized $GdVO_4$:Eu^{3+} was found to be well crystalline with tetragonal phase (JCPDS No. 17-0260) as shown in Figure 1a. The SEM micrograph (Fig. 1b) shows $GdVO_4$ particles with distinct rounded morphology. The HRTEM image of

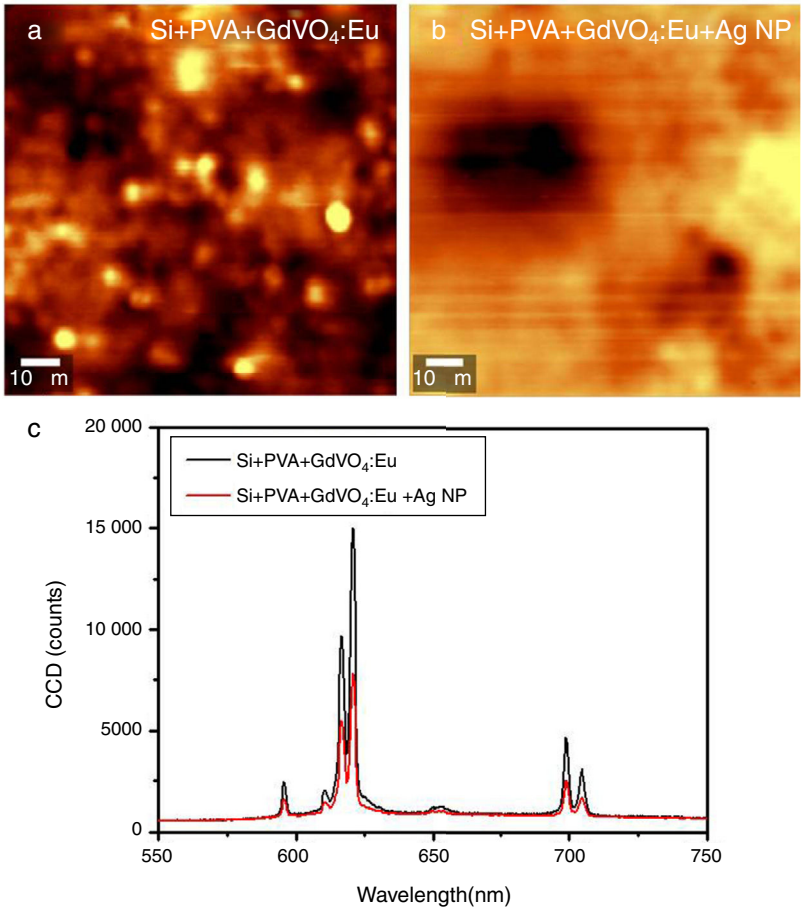

Fig. 5. Confocal fluorescence map of (a) PVA + $GdVO_4$:Eu; (b) PVA + $GdVO_4$:Eu + PVA + Ag NP deposited on the Si cell; (c)corresponding spectra comparing the Eu^{3+} emission intensity with and without Ag NPs suggesting quenching of fluorescence.

synthesized Ag nanoparticles displays that Ag nano prisms of average edge length 22 nm are formed as shown in Figure 1c.

The experimental UV-visible absorption spectra of Ag NP colloid (Fig. 2a) shows a sharp out-of-plane quadrupolar peak at 338 nm, an in-plane quadrupolar peak at 395 nm and a broad dipolar peak centered at 542 nm. The broadness of the absorption peak occurs because of the inhomogeneous damping caused by different spatial positions and random orientations of Ag NPs in the colloidal solution (Akselrod, Tischler, Young, Nocera, & Bulovic, 2010). The absorption spectra of the Ag nanoprisms cover the excitation range of $GdVO_4$:Eu^{3+} as revealed by the PL excitation spectra at the red emission of $GdVO_4$:Eu^{3+} (Fig. 2b), the charge transfer excitation band at 343 nm and digital photograph of $GdVO_4$:Eu^{3+} powder sample glowing red under UV excitation are shown in the inset of Figure 2b.

3.2. Photoluminescence

Confocal mapping of the four sets of samples namely (1) Si cell + $GdVO_4$:Eu^{3+} + AgNP; (2) Si cell + $GdVO_4$:Eu^{3+} + PVA + Ag NP; (3) Si Cell + PVA + $GdVO_4$:Eu^{3+} + Ag NP: (4) Si cell + PVA + $GdVO_4$:Eu^{3+} + PVA + Ag NP was done under the excitation of a UV diode laser (375 nm). The measurements on each set were done in the sequential order of layer formation, without disturbing the Si cell position on the microscope platform, keeping all the parameters the same so that the comparison of the emission intensity could be made after deposition of each layer in every set of samples and the optimum layer sequence exhibiting the maximum emission intensity could be determined.

After deposition of the $GdVO_4$:Eu^{3+} layer, characteristic sharp emission peaks corresponding to f-f transitions ($^5D_0$-^7F_J) of Eu^{3+} appeared with CCD counts in few thousands. In the first set of measurement, when a comparison was made in the emission intensity of the Si cell + $GdVO_4$:Eu^{3+} and Si cell + $GdVO_4$:Eu^{3+} + Ag NPs, it was observed that on addition of Ag NPs directly on the $GdVO_4$:Eu^{3+} layer, the emission was quenched to 0.82 times its original intensity as shown in the confocal fluorescence maps and the corresponding emission spectra in Figure 3.

In the second set, when a dielectric spacer layer of PVA was deposited between the $GdVO_4$:Eu^{3+} and Ag NPs, there occurred a significant enhancement (310%) in the emission intensity as shown in the same area fluorescence maps and spectra before and after deposition of the Ag NPs (Figure 4).

In the third set of measurements, when an additional layer of PVA was deposited between the Si cell and $GdVO_4$:Eu^{3+} but no spacer layer was deposited in between the emitting

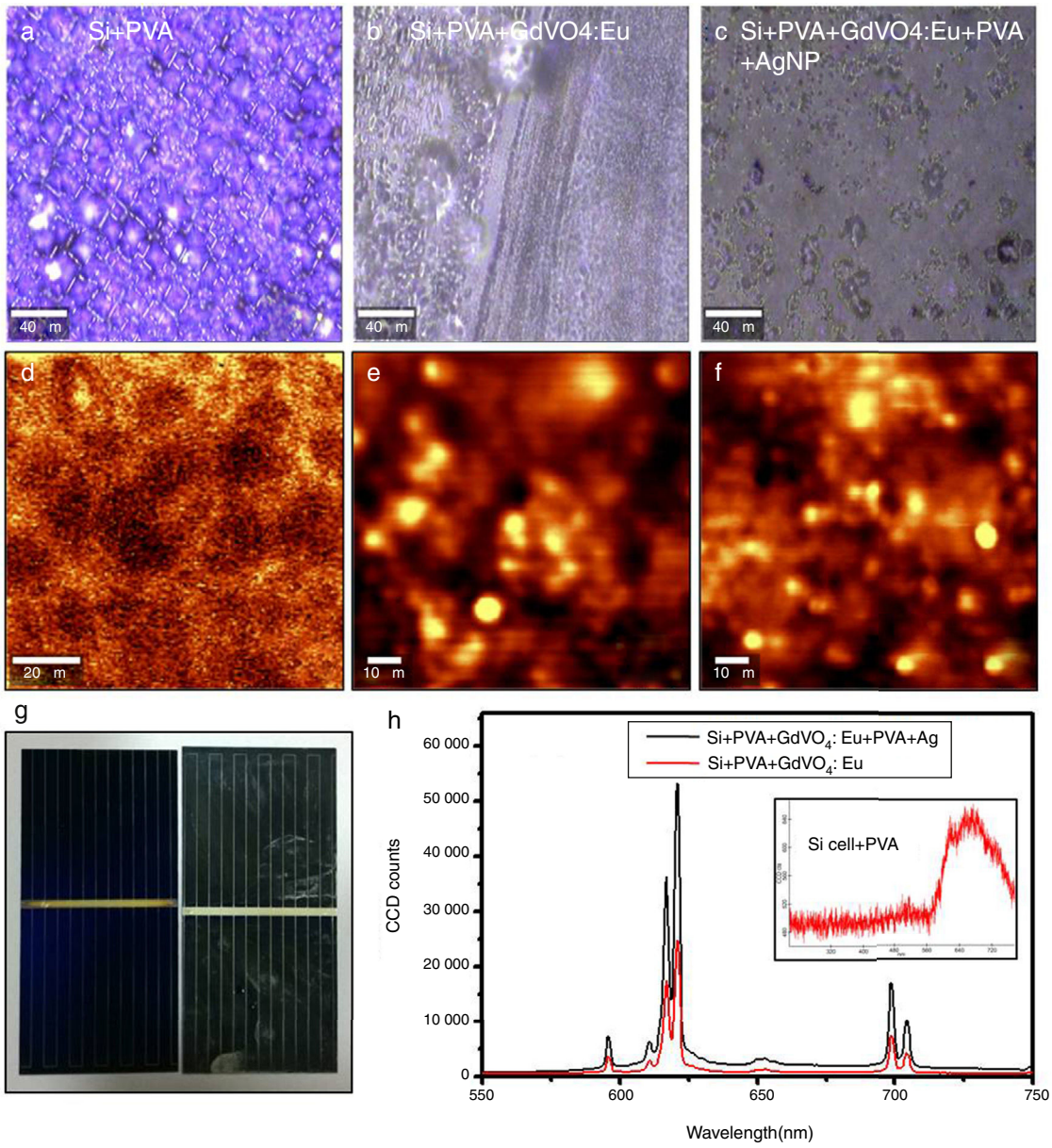

Fig. 6. Optical images and confocal fluorescence map of: (a) and (d), the Si Cell + PVA; (b) and (e), the Si cell + PVA + $GdVO_4$:Eu; (c) and (f), the Si cell + PVA + $GdVO_4$:Eu + PVA + Ag NP; (g), digital image of the bare Si cell (left) PVA + $GdVO_4$:Eu + PVA + Ag NP deposited on the Si cell; (h) corresponding spectra comparing the Eu^{3+} emission intensity with and without Ag NPs suggesting enhancement of fluorescence, the inset shows the emission from the Si cell with the PVA layer under the same experimental conditions.

species $GdVO_4$:Eu^{3+} and plasmonic field generating Ag NP layer, comparison was made between the emission intensities before and after Ag NP deposition. As seen in Figure 5, it is evidently discernible that because of the addition of Ag NPs, fluorescence quenching (0.53 times its original intensity) occurs. In the same configuration, when an intervening dielectric layer of PVA was employed between $GdVO_4$:Eu^{3+} & Ag NPs (set 4), an excellent increment (216%) in CCD counts was observed, as shown in the confocal fluorescence maps of the same area and the emission spectra in Figure 6. Optical images and the confocal fluorescence map are shown of Si Cell + PVA (Fig. 6a and d); Si cell + PVA + $GdVO_4$:Eu (Fig. 6b and e); Si cell + PVA + $GdVO_4$:Eu + PVA + Ag NP (Fig. 6c and f); digital image of the bare Si cell (left) and PVA + $GdVO_4$:Eu + PVA + Ag NP deposited on the Si cell (Fig. 6g); the corresponding spectra comparing the Eu^{3+} emission intensity with and without Ag NPs (Fig. 6h) suggest enhancement of fluorescence. Whereas the Bare Si cell gave emission spectra with a broad peak at 670 nm with maximum 150 CCD counts (Fig. 6h, inset). The results of the PL measurements are tabulated in Table 1, which clearly elucidates the fact that an intervening dielectric layer (PVA) between the emitter layer ($GdVO_4$:Eu^{3+}) and Ag NP layer is essential for the enhancement of red fluorescence from $GdVO_4$:Eu^{3+}.

According to reports (Lakowicz, Malicka, Huang, Gryczynski, & Gryczynski, 2004), a range of preferable distance from about 40 nm to about 200 nm between silver nanoparticles and fluorophore lead to metal enhanced

Table 1
Effect on Eu^{3+} red emission of conjugation process with Ag NPs on Si cell surface.

Sample No.	Layer sequence	Effect on fluorescence (ratio of emission intensity after and before Ag NP layer)
1	Si cell + $GdVO_4$:Eu^{3+} + AgNP	Quenching (0.82 times)
2	Si cell + $GdVO_4$:Eu^{3+} + PVA + Ag NP	Enhancement (3.10 times)
3	Si cell + PVA + $GdVO_4$:Eu^{3+} + Ag NP	Quenching (0.53 times)
4	Si cell + PVA + $GdVO_4$:Eu^{3+} + PVA + Ag NP	Enhancement (2.20 times)

fluorescence. Particularly, for the PVA spacer layer, enhanced photoluminescence and quantum yield have been observed from J-aggregate film separated by a 100 nm thick spin-coated layer of PVA (Geddes, 2013) from metal nanoparticles. For the present case, the deposited PVA spacer layer has a typical thickness of about 100 nm, as measured by an optical profilometry [Stylus Profilometer (Ambios XP200)]. The investigation on four sets of samples clearly exemplify that enhancement of fluorescence occurs only when there is a PVA spacer layer between the emitter (Eu^{3+} in $GdVO_4$ host) and Ag nanoprisms (sample set 2 and 4). When the PVA layer is placed in between the phosphor and Ag NPs, direct contact of the two species is averted which would have resulted in fluorescence quenching, favoring non radiative transitions from phosphor in contact with Ag NPs as observed for sample sets 1 and 3.

Metal-enhanced fluorescence occurs since highly localized electromagnetic (EM) fields generated around metal nanoparticles (MNP) by resonant excitation of conduction electrons in MNP (surface plasmons) as well as the lightening rod effect, which strictly depends on the shape of MNP, can augment fluorescence by excitation and/or emission enhancement. For such enhancement to take place, the excitation or emission spectra of phosphor must spectrally overlap with the plasmon absorption band of MNP. For the present case, the Ag NP absorption spectra show quadrupolar peaks at 338 nm and 395 nm and a broad dipolar peak centered at 542 nm (Fig. 2a), which falls in the excitation range of the phosphor $GdVO_4$:Eu^{3+} that exhibits broad charge transfer excitation band around 343 nm and sharp excitation peaks at 395 nm, 466 nm and 537 nm (Fig. 2b) because of direct excitation of Eu^{3+} ions. Moreover, the fluorescence enhancements and quenching observed in all the four sets of samples occur across all the characteristic $^5D_0$–^7F_J transitions in the orange to deep red-emission range of Eu^{3+} ions suggest an enhanced/decreased excitation of the phosphor particles from the plasmonic near field of Ag NPs due to the effect of layer sequence.

4. Conclusions

In order to achieve plasmon enhanced fluorescence on a single crystal Si solar cell, a comprehensive work on different sequence of deposition of layers of phosphor, metal nanoparticles and dielectric PVA layer on a commercial Si cell surface was carried out. The work involved chemical synthesis of shape tailored silver nanoprisms and Eu^{3+}-doped phosphor with extended excitation range to match the absorption range of Ag nanoparticles, conjugation of Ag NP and phosphor in various configurations to ensure the best sequence for fluorescence enhancement. Confocal fluorescence mapping and spectroscopy used to investigate the same area before and after Ag NP deposition unequivocally establish plasmonic enhancement of fluorescence on the commercial Si solar cell surface. Such fluorescence enhancements (up to 310%) of Eu^{3+} red emission is achievable only when an intervening PVA layer separates the emitter and the metal nanoparticles whereas a PVA layer between the Si cell surface and the emitter decreases fluorescence. Direct deposition of MNPs on the emitter quenches fluorescence, with more quenching with a PVA layer between the Si cell surface and the emitter. A decrease in enhancement and an increase in fluorescence quenching because of a PVA layer on the Si cell surface may probably be caused by the absorption/scattering of the emitted photons in the interlayer. As the down shifting phosphor layer has been reported to enhance solar cell efficiency, such plasmon-enhanced red emission from vanadates on a commercial single crystal Si solar cell holds promise for further performance enhancement of silicon PV devices.

Conflict of interest

The authors have no conflicts of interest to declare.

Acknowledgements

Author S.B thanks CSIR for providing SRF fellowship and Mr. Zubair Buch for the synthesis and characterization of Ag nanoprisms.

References

Akselrod, G. M., Tischler, Y. R., Young, E. R., Nocera, D. G., & Bulovic, V. (2010). Exciton-exciton annihilation in organic polariton microcavities. *Physical Review B*, *82*(11), 113106.

Anger, P., Bharadwaj, P., & Novotny, L. (2006). Enhancement and quenching of single-molecule fluorescence. *Physical Review Letters*, *96*(11), 113002.

Bishnoi, S., Das, R., & Chawla, S. (2014). Gold nanosphere enhanced green and red fluorescence in ZnO: Al, Eu^3+. *Applied Physics Letters*, *105*(23), 233108.

Buch, Z., Kumar, V., Mamgain, H., & Chawla, S. (2013). Silver nanoprisms acting as multipolar nanoantennas under a low-intensity infrared optical field exciting fluorescence from Eu^3+. *The Journal of Physical Chemistry Letters*, *4*(22), 3834–3838.

Geddes, C. D. 2013. Metal enhanced fluorescence-based sensing methods. US Patent No. US 20130102770 A9, Publication date April 25, 2013.

Chawla, S., Parvaz, M., Kumar, V., & Buch, Z. (2013). Fabrication of dual excitation dual emission phosphor with plasmonic enhancement of fluorescence for simultaneous conversion of solar UV and IR to visible radiation. *New Journal of Chemistry*, *37*(12), 3991–3997.

Kumar, V., Khan, A. F., & Chawla, S. (2013). Intense red-emitting multi-rare-earth doped nanoparticles of YVO4 for spectrum conversion towards improved energy harvesting by solar cells. *Journal of Physics D: Applied Physics*, *46*(36), 365101.

Chander, N., Sardana, S. K., Parashar, P. K., Khan, A. F., Chawla, S., & Komarala, V. K. (2015). Improving the short-wavelength spectral response of silicon solar cells by spray deposition of YVO 4: Eu 3+ downshifting phosphor nanoparticles. *IEEE Journal of Photovoltaics*, *5*(5), 1373–1379.

Yen-Chi, C., Woan-Yu, H., & Teng-Ming, C. (2011). Enhancing the performance of photovoltaic cells by using down-converting KCaGd (PO4) 2: Eu3+ phosphors. *Journal of Rare Earths*, *29*(9), 907–910.

Chen, Y. C., & Chen, T. M. (2011). Improvement of conversion efficiency of silicon solar cells using up-conversion molybdate $La_2Mo_2O_9$: Yb, R (R= Er, Ho) phosphors. *Journal of Rare Earths*, *29*(8), 723–726.

Dai, Q., Foley, M. E., Breshike, C. J., Lita, A., & Strouse, G. F. (2011). Ligand-passivated Eu:Y_2O_3 nanocrystals as a phosphor for white light emitting diodes. *Journal of the American Chemical Society*, *133*(39), 15475–15486.

El Daif, O., Tong, L., Figeys, B., Van Nieuwenhuysen, K., Dmitriev, A., Van Dorpe, P., . . ., & Dross, F. (2012). Front side plasmonic effect on thin silicon epitaxial solar cells. *Solar Energy Materials and Solar Cells*, *104*, 58–63.

Feng, W., Sun, L. D., & Yan, C. H. (2009). Ag nanowires enhanced upconversion emission of $NaYF_4$:Yb, Er nanocrystals via a direct assembly method. *Chemical Communications*, (29), 4393–4395.

Gavrilović, T. V., Jovanović, D. J., Lojpur, V., & Dramićanin, M. D. (2014). Multifunctional Eu^{3+}- and Er^{3+}/Yb^{3+}-doped $GdVO_4$ nanoparticles synthesized by reverse micelle method. *Scientific Reports*, *4*, 4209.

Guedje, F. K., Giloan, M., Potara, M., Hounkonnou, M. N., & Astilean, S. (2012). Optical properties of single silver triangular nanoprism. *Physica Scripta*, *86*(5), 055702.

Hao, E., & Schatz, G. C. (2004). Electromagnetic fields around silver nanoparticles and dimers. *The Journal of Chemical Physics*, *120*(1), 357–366.

Heredia, V. E. T. (2011). *Silver Nanostructures: Chemical Synthesis of colloids and composites nanoparticles, plasmon resonance properties and silver nanoparticles monolayer films prepared by spin-coating*. Barcelona, Catalonya: Universidad Politecnica de Catalunya., *Doctoral Thesis*, www.tdx.cat/bitstream/10803/52807/3/tveth1de1.pdf.

Huang, C. K., Chen, Y. C., Hung, W. B., Chen, T. M., Sun, K. W., & Chang, W. L. (2013). Enhanced light harvesting of Si solar cells via luminescent down-shifting using YVO_4:Bi^{3+}, Eu^{3+} nanophosphors. *Progress in Photovoltaics: Research and Applications*, *21*(7), 1507–1513.

Jayaramaiah, J. R., Lakshminarasappa, B. N., & Nagabhushana, B. M. (2012). Luminescence studies of europium doped yttrium oxide nano phosphor. *Sensors and Actuators B: Chemical*, *173*, 234–238.

Khan, A. F., Haranath, D., Yadav, R., Singh, S., Chawla, S., & Dutta, V. (2008). Controlled surface distribution and luminescence of YVO_4:Eu^{3+} nanophosphor layers. *Applied Physics Letters*, *93*(7), 073103.

Klampaftis, E., Congiu, M., Robertson, N., & Richards, B. S. (2011). Luminescent ethylene vinyl acetate encapsulation layers for enhancing the short wavelength spectral response and efficiency of silicon photovoltaic modules. *IEEE Journal of Photovoltaics*, *1*(1), 29–36.

Lakowicz, J. R., Malicka, J., Huang, J., Gryczynski, Z., & Gryczynski, I. (2004). Ultrabright fluorescein-labeled antibodies near silver metallic surfaces. *Biopolymers*, *74*, 467–475.

Le Donne, A., Acciarri, M., Narducci, D., Marchionna, S., & Binetti, S. (2009). Encapsulating Eu^{3+} complex doped layers to improve Si-based solar cell efficiency. *Progress in Photovoltaics: Research and Applications*, *17*, 519–525.

Liu, J., Wang, K., Zheng, W., Huang, W., Li, C. H., & You, X. Z. (2013). Improving spectral response of monocrystalline silicon photovoltaic modules using high efficient luminescent down-shifting Eu^{3+} complexes. *Progress in Photovoltaics: Research and Applications*, *21*(4), 668–675.

Richards, B. S. (2006). Luminescent layers for enhanced silicon solar cell performance: down-conversion. *Solar Energy Materials and Solar Cells*, *90*(9), 1189–1207.

Shalav, A., Richards, B. S., Trupke, T., Krämer, K. W., & Güdel, H. U. (2005). Application of $NaYF_4$:$Er^{3+}$$NaYF_4$:$Er^{3+}$ up-converting phosphors for enhanced near-infrared silicon solar cell response. *Applied Physics Letters*, *86*(1), 013505.

Singh, N. S., Ningthoujam, R. S., Phaomei, G., Singh, S. D., Vinu, A., & Vatsa, R. K. (2012). Re-dispersion and film formation of $GdVO_4$:Ln^{3+} (Ln^{3+} = Dy^{3+}, Eu^{3+}, Sm^{3+}, Tm^{3+}) nanoparticles: particle size and luminescence studies. *Dalton Transactions*, *41*(15), 4404–4412.

Thouti, E., Sharma, A. K., Sardana, S. K., & Komarala, V. K. (2014). Internal quantum efficiency analysis of plasmonic textured silicon solar cells: surface plasmon resonance and off-resonance effects. *Journal of Physics D: Applied Physics*, *47*(42), 425101.

Wan, D., Chen, H. L., Tseng, T. C., Fang, C. Y., Lai, Y. S., & Yeh, F. Y. (2010). Antireflective nanoparticle arrays enhance the efficiency of silicon solar cells. *Advanced Functional Materials*, *20*(18), 3064–3075.

Wang, Q., Song, F., Lin, S., Liu, J., Zhao, H., Zhang, C., . . ., & Pun, E. Y. (2011a). Optical properties of silver nanoprisms and their influences on fluorescence of europium complex. *Optics express*, *19*(8), 6999–7006.

Wang, Q., Song, F., Lin, S., Ming, C., Zhao, H., Liu, J., . . ., & Pun, E. Y. (2011b). Effect of silver nanoparticles with different shapes on luminescence of samarium complex at two different excitation wavelengths. *Journal of Nanoparticle Research*, *13*(9), 3861–3865.

Yadav, R., Khan, A. F., Yadav, A., Chander, H., Haranath, D., Gupta, B. K., . . ., & Chawla, S. (2009). Intense red-emitting $Y_4Al_2O_9$:Eu^{3+} phosphor with short decay time and high color purity for advanced plasma display panel. *Optics Express*, *17*(24), 22023–22030.